A bioeconomic MPA study based on cellular automata population growth and distribution

by Arne Eide

Norwegian College of Fishery Science, University of Tromsø

email: arne.eide@nfh.uit.no

Abstract

This paper investigates possible biological and economic effects by the use of marine protected areas (*MPAs*) as a management tool, employing cellular automata (*CA*) techniques to model biological growth and area distribution. Two simple *2D* continuous cellular automata (*CCA*) models are presented and incorporated in a fish harvest model based on standard assumptions of economic rational behaviour by individual decision makers with free access to a common-pool fish stock resource. Stock dynamics is modelled as a discrete process in time and area. Performance of *MPA* regulations has been studied under different diffusion and growth conditions and different types of effort distribution. As expected the *MPA* regulation performance is found to be strongly linked to the size of the protected area and the diffusion properties of the stock. First of all the year to year fluctuation in the state variables proves to be functions of the size of the protected area.

Keywords: Bioeconomics, Marine Protected Area, Cellular automata

Introduction

As the word suggests, the aim of a Marine Protected Area is to protect marine ecosystems from human activities which may cause destruction or other unwanted impact on the environment or species located in the area. Such destruction may have negative economic consequences for fisheries, tourism or other industries. In this study the MPA area defines a region where fishing activities are prohibited, while there is open access to the fish resource outside the MPA area. The term MPA is chosen because it is commonly used in the literature, but the only type of MPA considered in this study is marine sanctuaries.

A vast number of publications on the economics of fisheries managed by *MPA* have emerged the last years. The papers do however not give a unanimous answer on what value *MPA* regulation has as a management measure. Several studies based on deterministic models indicate that *MPA* in fact has limited value as a management tool (Hannesson 1998; Conrad 1999). The introduction of *MPA* simply reduces the net revenues, and the conservation effect is weak unless very large areas are included in the marine sanctuary. Conrad (1999) argues that deterministic models are less useful to reveal the true value of *MPA* regulation. He therefore introduced a model with stochastic growth and found the variance of fish stock biomass to be reduced by the introduction of marine sanctuaries. Hannesson (2002) arrived at the same conclusion using a stochastic spatial distribution of the stock components inside and outside the *MPA*.

The spatial component seems to be the methodological most challenging problem while investigating economic effects of *MPA* regulation. A variety of different models exists, but the most common approach is to define two stock components, one within the *MPA* and the other within the fishable area, where both areas interact through density driven migration. Different solutions exist on how to handle the environmental carrying capacity of two stock components and differences in conclusions seem in some extent to reflect differences in methodology. Such models are specified in

continuous time or as discrete processes in time and they are used both to investigate open access solutions and maximizing present value of net revenues over time.

Sumaila and Charles (2002) give a useful introduction to different approaches to economic modelling of fisheries in the presence *MPAs*. According to the different classes of models identified by Sumaila and Charles (2002), this study should be categorised as a theoretical study on behavioural economics in a deterministic spatially-heterogeneous model including *MPA*. The idea presented in this paper is to use a deterministic spatially-heterogeneous model based on the principles of cellular automata modelling combined by a more traditional harvest production model under the assumptions of open access to the stock resources.

Moustakas et al. (2006) developed a high resolution migratory fish and fishers model including stochastic elements, for evaluating effects of closed areas. Fishing is included as a learning process by vessel movements between neighbouring cells based of fish stock densities. Apart from harvest production economic modelling is not included and the fleet dynamics is controlled by presence of fish, willingness to move and fleet density constraints. Moustakas et al. (2006) utilised cellular automata methodology to model spatial distribution in the model.

Cellular automata methodology (Wolfram 2002) is a rather new approach to model a variety of complex systems by certain arbitrary rules specifying how the automaton develops. The cellular automaton consists of cells and the state of each cell evolves over time due to rules based on current state of the cell and its neighbouring cells. Simple rules may create extremely complex pattern as the automaton defined by a fixed number of cells evolves from one computational stage to the next. The original idea of cellular automata (*CA*) presented by Wolfram in the early 1980ies was a dynamic model, discrete in time (stages of evolvement), space and state. The basic idea is not altered by modifying the original model to include a continuous state variable within each cell, normally referred to as continuous cellular automata (*CCA*; see Wolfram 2002).

Darwen and Green (1996) claims that cellular automata methodology is a better approach than partial differential equations to model a population in a landscape. *CA* and *CCA* models are consistent with empirical experiences in allowing population density to be heterogeneous, with local extinctions and local booms (Darwen ad Green 1996). The simplicity of cellular automata also reduces the computer time compared with corresponding models based on solving differential equations.

Balzer et al. (1998) gives a good overview over the first two decades of the development of cellular automata ecological models. During recent years the number of publications within this field has exploded and cellular automata models are now virtually covering all areas of biological modelling as well as most other modelling areas.

The models presented in this paper are deterministic models where the fish stock biomass essentially develops by simple *CCA* rules, also influenced by fishing activities. The fleet dynamics is a function of economic performance, following standard open access dynamics where the growth in fishing effort is proportional to net revenue.

This study includes two alternative biological growth models, both based on continuous cellular automata modelling. The first (referred to as *CCA*) is a model presented by Wolfram (2002; page 157), while the other (referred to as *LCA*) is a straight forward cellular automata representation of a discrete time logistic growth equation. A slightly altered logistic growth model was also studied as a cellular automata rule by Darwen and Green (1996). Their model included however a grid of cells (lattice of sites) while the models presented here consist of a row of cells evolving over discrete computational steps.

Biological model

Assume a linear representation of a fish stock biomass distribution. Total stock biomass is the sum of discrete biomasses along the line in a finite number (n) of biomass cells. Let the first and last cell at the line connect to each other similarly as two neighbouring cells, converting from a linear to a circular cell distribution. The initial biomass vector with n elements is

$$\mathbb{b} = (b_1, b_2, b_3, \ldots., b_n). \tag{1}$$

$\mathbb{b}$ evolves over time as a function of $\mathbb{b}$ and a simple CA rule involving a growth rate (g) and a fixed diffusion pattern. The diffusion pattern is given by the range parameter r which determines the range of the rule in number of affected neighbouring cells at each side of the actual cell (Wolfram, 1984). In case of $r = 1$ the biomass origin from b_2 in (1) the next time step will be distributed equally to b_1, b_2 and b_3. In the first model (*CCA*) only the fractional part of the new biomass will remain in the cell, therefore

$$0 \le b_i \le 1 \tag{2}$$

for $1 \le i \le n$. The growth rate (g) gives the percentage growth per unit of time. The biomass growth is then expressed by

$$b_{i,t+1} = \text{frac}\left(\frac{g+1}{2r+1}\sum_{j=i-r}^{i+r} b_{j,t}\right), \tag{3}$$

while $b_{n+1,t} = b_{1,t}$, $g \ge 0$ and $r \ge 0$.

Natural mortality is expressed indirectly by the remaining fractional part, assuming a density dependent mortality. The biomass vector is a discrete function of time at given initial biomass value ($\mathbb{b}_0$), here expressed by the continuous cellular automata rule

$$\mathbb{b}_t = \mathrm{CCA}(\mathbb{b}_{t-1}). \tag{4}$$

The corresponding discrete logistic growth equation is

$$b_{i,\,t+1} = \frac{g+1}{2\,r+1}\left(1 - 2\sum_{j=i-r}^{i+r} b_{j,t}\right)\sum_{j=i-r}^{i+r} b_{j,t}, \tag{5}$$

represented by the cellular automata rule

$$\mathbb{b}_t = \mathrm{LCA}(\mathbb{b}_{t-1}). \tag{6}$$

Total biomass at time t is

$$B_t = \sum_{i=1}^{n} b_{i,\,t}. \tag{7}$$

According to Wolfram (2002) the equilibrium biomass is $B_\infty = \frac{n}{2}$ for $r > 0$. Biomasses calculated by Model (4) are presented in Table 1 for 13 cells, $g = \frac{1}{2}$ and an initial biomass with value 1 placed in the mid cell. Table 2 displays corresponding biomasses of Model (6) distributed on 7 cells and $g = \frac{3}{5}$.

Graphical examples of the biological model (4) are shown in figures 1 and 2 for two different initial conditions, while varying growth rate (g) and diffusion pattern (r). Figure 1 shows how a single initial biomass in the centre cell of 99 cells develops over 100 time steps for different growth and range parameters, as shown numerically in Table 1. In Figure 2 the initial condition is a fixed seed random initial biomass distribution on 100 horizontal cells in the first (upper) row.

Growth model (4) is displayed in Figures 1 and 2 as biomass patterns, while Figures 3-5 present biomass development over time (B_t) in a more traditional way. Corresponding biomass developments shown as biomass surfaces or patterns in Figure 2 are presented as biomass curves in Figure 3. The figures show how diffusion and growth properties affect biomass variations. The development of 100 cells with low growth rates is in Figure 2 seen as pattern stretched in the vertical direction, while increasing ranges stretches the pattern in the horizontal direction.

While increasing number of cells (n) and time span (t), the graphical presentation displayed in Figures 1 and 2 soon turns useless and more traditional graphical presentations of stock biomass development over time prove to be more useful. Figure 3 reveals both a lower biomass in the case of $r = 0$ and $g = 0.25$, while increased biomass fluctuations occur by increased r-values. These fluctuations seem to be damped by increasing growth rates (g). An interesting difference between Models (4) and (6) is the lower equilibrium biomass in the first in case of $r = 0$.

From a biological point of view diffusion may be explained as adaptation to environmental conditions, as prey density may increase and predator density decline by migratory behaviour. The principal difference is found between diffusion ($r > 0$) and no diffusion ($r = 0$), since the range parameter (r) value defines the speed of adaptation. A full investigation of the growth and range properties of the two models are however not included in this study.

Figures 4 and 5 show the biomass growth curves of Models (4) and (6) when initial cell biomasses are low. Figure 4 displays total biomass development over time with a spatial distribution on 100 cells, while Figure 5 displays the corresponding picture in the case of 100,000 cells. The impacts of increasing growth rates and range of rules (diffusion) are easily seen in both figures. The solid curves represent the *CCA* model, while th dashed curves represent the logistic growth model (*LCA*).

Increasing the number of cells creates smoother curves, as seen while comparing Figures 4 and 5. Increased diffusion increases biomass fluctuation, while mean biomass equilibrium remains independent of diffusion properties, with the previously mentioned exception of no diffusion (r = 0), leading to significant lower average total biomass.

Model (4) and (6) express biomass growth as discrete time processes on micro levels (within and between cells). Total biomass is not a variable in the growth functions at micro level, but in the long run the average biomass of neighbouring cells may be a good proxy of the overall total biomass in the stock in the absence of harvest. Diffusion (represented by range parameter r) increases each cell's impact on neighbouring cells and may contribute in establishing a closer relationship between micro biomasses (in cells) and total biomass.

Fishing regulated by closed area

Let us now introduce fishing to the biological models (*CCA* and *LCA*) presented above. The only fishing activity regulation is by the closed *MPAs*. The control is assumed to be perfect and no control costs are considered.

The stock biomass within a *MPA* is given as a subset of the biomass vector $\mathbb{b}$,

$$\mathbb{b}_{\text{MPA}} = (b_s, \ ...., \ b_{s+m-1})$$

where s is the first cell and m is the number of cells included in the *MPA*. Absence of protected area is regarded being a special case of *MPA* regulation (no closed area; $m = 0$). The model circularity makes the choice of s-value unimportant, hence $s = 1$ is used in the following. The *MPA* biomass vector then simplifies to

$$\mathbb{b}_{\text{MPA}} = (b_1, \ ...., \ b_m), \tag{8}$$

$$0 \le m \le n.$$

Fishing activities target biomasses in the non-protected area (*NPA*), represented by the complementary subset to $\mathbb{b}_{\mathrm{MPA}}$ of the biomass vector $\mathbb{b}$

$$\mathbb{b}_{\mathrm{NPA}} = (b_{1+m}, \ldots, b_n). \tag{9}$$

Total targeted biomass at time t then is

$$B_{\mathrm{NPA},t} = \sum_{i=1+m}^{n} b_{i,t}. \tag{10}$$

Most harvest production models assume a priori the stock-output elasticity to equal one. This origins from the basic assumption of a linear relationship between the fishing mortality rate and the fishing effort per unit of time. Most studies on stock-effort-harvest relationships indicate however that this linear relationship is rare, as the stock-output elasticities normally is found to be well below 1, most often closer to 1/2 than to 1 (Hannesson 1983; Eide et al. 2003). The fish harvest production function used in this study therefore assumes a stock output elasticity of 1/2, while harvest (h) is assumed to be linear in fishing effort;

$$h_{i,t} = q\, e_{i,t} \sqrt{b_{i,t}}\,, \tag{11}$$

when $b_i \in \mathbb{b}_{\mathrm{NPA}}$ and e_i is the fishing effort of cell i. Total fishing effort is the sum of the fishing effort of all cells

$$E_t = \sum_{i=1+m}^{n} e_{i,t} \tag{12}$$

and total harvest is given by

$$H_t = \sum_{i=1+m}^{n} h_{i,t}\,. \tag{13}$$

The spatial dimension in the cellular automaton opens for different ways of spatial distribution of fishing effort. A distribution rule based on stock biomass distribution is given by the expression

$$e_{i,t} = \frac{{b_{i,t}}^d}{\sum_{i=1+m}^{n} {b_{i,t}}^d} E_t, \tag{14}$$

where the distribution parameter d (normally $d \geq 0$ is expected) controls to what extent biomass distribution affects the distribution of fishing effort. The special case $d = 0$ gives a homogenous distribution of fishing effort independent of biomass distribution. This rule covers most published *MPA* models separating the stock into two components. Fishing effort per cell with homogenous distribution ($d = 0$) is constant, equal

$$e_{i,t} = \frac{{b_{i,t}}^0}{\sum_{i=1+m}^{n} {b_{i,t}}^0} E_t = \frac{E_t}{n-m}, \tag{15}$$

while $d = 1$ gives an effort distribution perfectly reflecting the stock biomass distribution. $d > 1$ represents effort distributions which take advantage of biomass clustering, successfully targeting cells with the highest biomass densities. The extreme is of course $d = +\infty$, by which all fishing effort is placed in the single cell holding the highest biomass.

More sophisticated distribution rules (or simple cellular automatons, for example as proposed by Moustakas et al., 2006) may take into consideration distribution histories (of biomass and effort) and put constraints on local densities and growth of effort. The distribution model proposed above

(equations 14) connects however to history through the total fishing effort path over time, as will be explained in the next section.

Including harvest model (11) in the biological growth model (3) yields

$$b_{i,\,t+1} = \text{frac}\left(\frac{g+1}{2\,r+1}\sum_{j=i-r}^{i+r} b_{j,t}\right) - h_{i,t} \tag{16}$$

Equation (4) is adjusted accordingly and the complete *CCA* model including harvest (by the fishing effort *E*) and *MPA* regulation (by the MPA size variable *m*), is expressed by

$$\mathbb{b}_t = \text{CCA}(\mathbb{b}_{t-1},\, E_{t-1},\, m_{t-1},), \tag{17}$$

m being the number of *MPA* cells and *E* the total fishing effort. Corresponding expression in the logistic case is from equation (5) found to be

$$b_{i,\,t+1} = \frac{g+1}{2\,r+1}\left(1 - 2\sum_{j=i-r}^{i+r} b_{j,t}\right)\sum_{j=i-r}^{i+r} b_{j,t} - h_{i,t} \tag{18}$$

and rule (6) is modified correspondingly,

$$\mathbb{b}_t = \text{LCA}(\,\mathbb{b}_{t-1},\, E_{t-1},\, m_{t-1},). \tag{19}$$

Economic model

The harvest equation (11) involves fishing effort (*E*) which is assumed to have a fixed unit cost *c*. The unit cost *c* also includes opportunity costs of all input factors in the production of fishing effort. Similarly a constant unit price of harvest (*p*) is assumed. The net revenue of harvest (*NR*) is

$$NR = p\,H \;-\; c\;E. \tag{20}$$

Since a normal profit is included in the unit cost of effort, *NR* more precisely is the total resource rent obtained in the fishery.

In an ongoing open access fishery current fishing effort is as a function of previous fishing effort and economic rent. Since normal profit already is included in the total cost of effort, normal profit is obtained from the harvest production process when $NR = 0$. Economic rent is earned when $NR > 0$, which with access to the common-pool resource should increase fishing effort. In this study effort dynamics is modelled while assuming a linear relationship between *NR* and change in effort, as a discrete time process;

$$E_{t+1} = E_t\,(1 + a\,NR_t). \tag{21}$$

a is the adjustment (stiffness) parameter and represents an intrinsic rate of change in effort. Cost of fishing effort (c) is decomposed on cells by fishing effort (equation 14), and net revenue of the cell, hence net revenue (economic rent) of cell i is

$$nr_i = p\,h_i - \frac{c\,{b_i}^d}{\sum_{i=1+m}^{n} {b_i}^d}\,E \tag{22}$$

or simply

$$nr_i = p\,h_i - \frac{E}{n-m} \tag{23}$$

in case of $d = 0$ (as seen from equation 15). Global net revenue is

$$NR = \sum_{i=1}^{n} nr_i. \tag{24}$$

Results

The biological models presented above (*CCA* and *LCA*, equations 17 an 19) include the biological and spatial parameters g, r, d and n. The economic part of the bioeconomic model includes the economic parameters q, p, c and a, while m is the management variable. The two state variables (biomass vector $\mathbb{b}$ and E) have initial values $\mathbb{b}_0$ and E_0.

Figures 6 and 7 display how fishing effort (horizontal axis) develops as economic rent (vertical axis) changes over time in Models (17) and (19) respectively, for different *MPA* regimes (in term of sizes). Parameter values used in the simulations presented by the two figures are shown in Table 3. The initial biomass vector in all simulations includes 100 cells evolving over 2000 time steps.

The ranges of the axes in the graphs displayed in Figure 6 are Total fishing effort (E) from 0 to 60 and economic rent (*NR*) from -250 to 150, while the corresponding ranges of the graphs in Figure 7 are from 0 to 15 (E) and from -20 to 20 (*NR*).

Figure 8 includes four value combinations of r and d (0 - 0, 2 - 0, 2 - 1 and 2 - 8) and average values of biomass, harvest, effort and rent, over a period of 500 time steps plotted on percentage area covered by *MPA*. The first column ($r = 0$, $d = 0$) is the situation of no migration between cells and homogenous distribution of fishing effort. The three columns to the right have all the same biological distribution range as in Figures 6 and 7 ($r = 2$). The second column represents the situation of homogenous distribution of effort ($d = 0$, as in the upper panels of Figures 6 and 7), next column (second column from the right) represents a distribution of fishing effort perfectly reflecting the distribution of biomass on cells ($d = 1$), while the right column represent an effort distribution effectively targeting cells of high biomass density ($d = 8$, as in the lower panels of Figures 6 and 7).

Figure 9 displays biomass surfaces as function of time and MPA size, referring to the biomasses shown in the first row of Figure 8. The second row of Figure 9 also connects to the upper panels in Figures 6 and 7, while the last row in Figure 9 connects to the lower panels of Figures 6 and 7.

A cluster analysis has been performed on the same data sets displayed in Figures 8 and 9. The results of the cluster analysis are shown in Figure 10 as dendrogram plots of data sets of different *r*-*d*-combinations for the *CCA* model (upper panel) and the *LCA* model (lower panel). Size of MPA is used as clustering variable.

Discussion

Figure 8 clearly shows increased average stock biomass by increased *MPA* size in an open access fishery. This is the case in both the *CCA* and *LCA* model. Biomass variance (only shown in Figure 8 for the *CCA* model 17) however is decreasing by increasing the *MPA* size, suggesting larger stock biomass fluctuations by smaller *MPA*s. This is consistent with the findings in the stochastic model presented by Conrad (1999), where also the difference in variance between open and closed area is discussed.

The decreasing variance related to increasing *MPA* size is reflected by average harvest (Figure 8) and first of all average net revenue (resource rent). Fleet dynamics related to net revenue fluctuations causes limit-cycle patterns in the *LCA* model (19) (see Figure 7), while the *CCA* model (17) shows pseudo-random patterns (Figure 6). The differences are also easily seen from the biomass surfaces of Figure 9, where decreasing fluctuations by increasing *MPA* sizes are illustrated. Furthermore Figure 7 displays increasing range of fishing effort within the limit-cycle while increasing *MPA* size up to a certain point (about 25% *MPA*), from which the opposite relation is found. Figure 6 may indicate a similar pattern in the *CCA* model (17).

The two figures (Figures 6 and 7) also show interesting differences in open access efforts between the two panels ($d = 0$ and $d = 8$) of each figure. In the lower panels ($d = 8$) fishing activities effectively targeting high density areas aim to maintain a high total production of fishing effort even when the size of *MPA* increases, while homogenous distribution of fishing effort ($d = 0$) produces larger fluctuations, but lower average fishing effort in open access. For the *CCA* model (Figure 6)

this is also reflected in Figure 8, where fluctuations over time are represented by confidence intervals (shaded areas), becoming more narrow as the *MPA* size increases.

Another interesting difference between the *CCA* and *LCA* models is found in the case of no biomass diffusion between cells ($r = 0$); easily seen in Figure 3 where biomass equilibrium of the *CCA* model never reaches the level of 0.5 times number of cells, while this is established by the *LCA* model. Increasing growth rate (g) moves however the *CCA* equilibrium biomass closer to the *LCA* equilibrium. The *LCA* model also shows to be more robust towards changes in d (Figure 8), while the *CCA* model displays significant changes as the value of d vary, reflecting more heterogeneous biomass distribution. While effort perfectly reflects biomass distribution ($d = 1$) average biomasses in the *CCA* model are very close to what is obtained by the *LCA* model. For other values of d the *CCA* biomasses seem however to always be larger of corresponding *LCA* biomasses. The conservation effect of MPA regulation therefore comes out to be less (and sometimes almost negligible) in the *CCA* model compared with the *LCA* model. With no MPA regulation or very small protected areas the result may however be opposite, as best seen from the biomass surfaces shown in Figure 9. Higher expertise in targeting the biomass clusters ($d > 0$) contributes in stabilising the stock and reducing the risk of depleting the stock by increasing values of d. Note that this result is corrected for the increased net revenue obtained by targeting higher densities of fish.

The positive resource rent obtained in open access fishery (as seen from Figures 6, 7 and in particular from Figure 8) may be surprising given the expected $NR = 0$. It is however well known that stock biomass fluctuations and fleet dynamics in the long run often lead to such effects (Eide, 2007). As the fluctuations are reduced by increased *MPA* size, the result is diminishing aggregated resource rent by increasing *MPA* size.

The cluster analysis displayed in Figure 10 shows that no clear pattern could be obtained identifying efficient *MPA* sizes. In the *CCA* model (upper panel) no *MPA* (0) shows to be significantly different from all other sizes of *MPA* (for $r = 2$ and d equal 0 or 1), while this is not equally apparent when d

= 8 or in within the *LCA* model. The latter model (lower panel) identifies other significantly different sets for other sizes of *MPA* (70% for $r = 0$, $d = 0$; 15% for $r = 2$, $d = 0$; 60% for $r = 2$, $d = 1$)

The concept of cellular automata represents a simple way of modelling spatial distributions. A range of alternative methods could be used to obtain this, and a number of previous MPA studies have utilised these methods. The other special feature of cellular automata modelling is however not equally easy achieved by other modelling techniques. Cellular automata implements micro dynamics at cell levels and is a bottom-up modelling approach. The biological models proposed in this study could also include cell specific parameter values in addition to the state variables. Varying environmental capacity of different cells could be implemented by varying cell specific growth rates and/or saturation levels (biomass maximum). A further study of the robustness of MPA regulation under different environmental conditions and distributions rules should also include spatial environmental variation. The model set up presented in this study represents a way forward to perform such investigations.

References

Balzer, Heiko, P.W. Braun and W. Köhler (1998). Cellular automata models for vegetation dynamics. Ecological Modelling 107:113-125.

Conrad, Jon (1999). The Bioeconomics of Marine Sanctuaries. Journal of Bioeconomics 1:205-217.

Darwen, P.J. and D.G. Green (1996). Viability of populations in a landscape. Ecological Modelling 85:165-171.

Eide, Arne (2007). Economic impacts of global warming: The case of the Barents Sea fisheries. Natural Resource Modeling, 20(2): 199-221.

Eide, Arne, Frode Skjold, Frank Olsen and Ola Flaaten (2003). Harvest Functions: The Norgwegian Bottom Trawl Cod Fisheries. Marine Resource Economics, 18:81-93.

Hannesson, Rögnvaldur (1983). Bioeconomic Production Functions in Fisheries: Theoretical and Empirical Analysis. Canadian Journal of Fish and Aquatic Science 40:969-982.

Hannesson, Rögnvaldur (1998). Marine Reserves: What Would They Accomplish? Marine Resource Economics 13:159-170.

Hannesson, Rögnvaldur (2002). The Economics of Marine Reserves. Natural Resource Modeling 15(3):273-289.

Moustakas, A., W. Silvert and A. Dimitromanolakis (2006). A spatially explicit learning model of migratory fish and fishers for evaluating closed areas. Ecological Modelling 192:245-258.

Sumaila, U. R. and A. Charles (2002). Economic Models of Marine Protected Areas: An Introduction. Natural Resource Modeling, 15(3):261-272.

Wolfram, Stephen (1984). Universality and Complexity in Cellular Automata. Physica 10D:1-35.

Wolfram, Stephen (2002). A new kind of science. Wolfram media, Champaign, IL.

Table 1. Cellular biomasses calculated by Model (4) for $g = 1/2$, $r = 1$ and $\mathbb{b}_0$ given by the first row (t =

first period of the pattern shown in the mid column of the first row of figure 1.

	b_1	b_2	b_3	b_4	b_5	b_6	b_7	b_8	b_9	b_{10}	b_{11}	b_{12}	b_{13}	B
t=0	0	0	0	0	0	0	1	0	0	0	0	0	0	1
t=1	0	0	0	0	0	$\frac{1}{2}$	$\frac{1}{2}$	$\frac{1}{2}$	0	0	0	0	0	$\frac{3}{2}$
t=2	0	0	0	0	$\frac{1}{4}$	$\frac{1}{2}$	$\frac{3}{4}$	$\frac{1}{2}$	$\frac{1}{4}$	0	0	0	0	$\frac{9}{4}$
t=3	0	0	0	$\frac{1}{8}$	$\frac{3}{8}$	$\frac{3}{4}$	$\frac{7}{8}$	$\frac{3}{4}$	$\frac{3}{8}$	$\frac{1}{8}$	0	0	0	$\frac{27}{8}$
t=4	0	0	$\frac{1}{16}$	$\frac{1}{4}$	$\frac{5}{8}$	0	$\frac{3}{16}$	0	$\frac{5}{8}$	$\frac{1}{4}$	$\frac{1}{16}$	0	0	$\frac{33}{16}$
t=5	0	$\frac{1}{32}$	$\frac{5}{32}$	$\frac{15}{32}$	$\frac{7}{16}$	$\frac{13}{32}$	$\frac{3}{32}$	$\frac{13}{32}$	$\frac{7}{16}$	$\frac{15}{32}$	$\frac{5}{32}$	$\frac{1}{32}$	0	$\frac{99}{32}$
t=6	$\frac{1}{64}$	$\frac{3}{32}$	$\frac{21}{64}$	$\frac{17}{32}$	$\frac{21}{32}$	$\frac{15}{32}$	$\frac{29}{64}$	$\frac{15}{32}$	$\frac{21}{32}$	$\frac{17}{32}$	$\frac{21}{64}$	$\frac{3}{32}$	$\frac{1}{64}$	$\frac{297}{64}$

Table 2. Cellular biomasses calculated by Model (6) for $g = 3/5$, $r = 1$ and $\mathbb{b}_0$ given by the first row (t =

	b_1	b_2	b_3	b_4	b_5	b_6	b_7	B
t=0	0	0	0	1	0	0	0	1
t=1	0	0	$\frac{2}{5}$	$\frac{2}{5}$	$\frac{2}{5}$	0	0	$\frac{6}{5}$
t=2	0	$\frac{24}{125}$	$\frac{128}{375}$	$\frac{56}{125}$	$\frac{128}{375}$	$\frac{24}{125}$	0	$\frac{568}{375}$
t=3	$\frac{7616}{78\,125}$	$\frac{832}{3375}$	$\frac{833\,152}{2\,109\,375}$	$\frac{912\,448}{2\,109\,375}$	$\frac{833\,152}{2\,109\,375}$	$\frac{832}{3375}$	$\frac{7616}{78\,125}$	$\frac{4\,030\,016}{2\,109\,375}$

Table 3. Parameter values used in the simulations displayed in Figures 6 and 7.

Paramet˙.	CCA	LCA	Comment
t	2000	2000	Number of time steps
n	100	100	Number of cells in population
r	2	2	Number of affected
g	0.5	0.5	Biological growth rate
$\mathbb{b}_0$	Seed random	Seed random	Initial cell biomass vector
E_0	5	5	Initial fishing effort
d	0 and 8	0 and 8	Fishing effort distribution parameter
q	1	1	Catchability coeffisient
p	10	10	Unit price of harvest
c	5	5	Unit cost of effort
a	0.002	0.002	Growth rate in effort dynamics

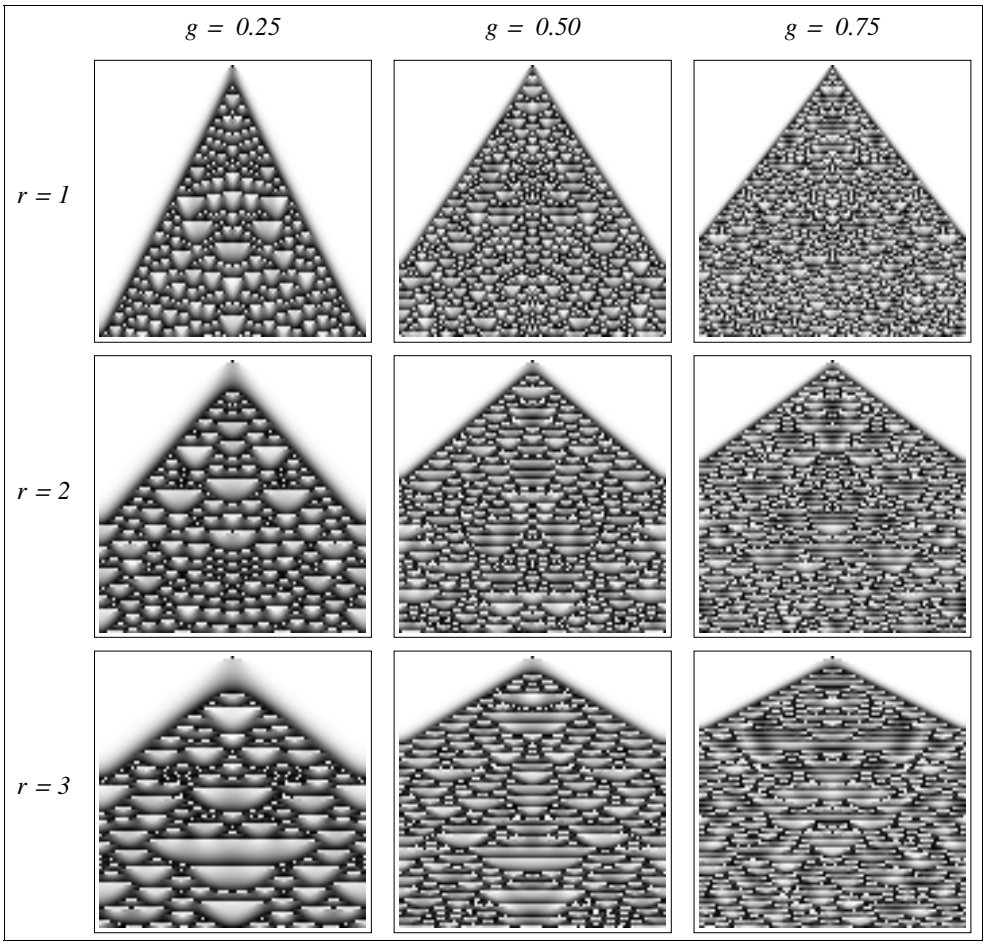

Figure 1. CCA model (4) of varying diffusion properties at constant growth with an initial condition of one single biomass (b_{49}=1) in the centre cell of 99 cells (n = 99). The growth rate (g) is 0.5 and the diffusion property given by the range parameter r , indicating number of influenced neighbouring cells. The vertical axes of each case represents computational steps (time), increasing downwards. The figure includes 100 computational steps (t=100).

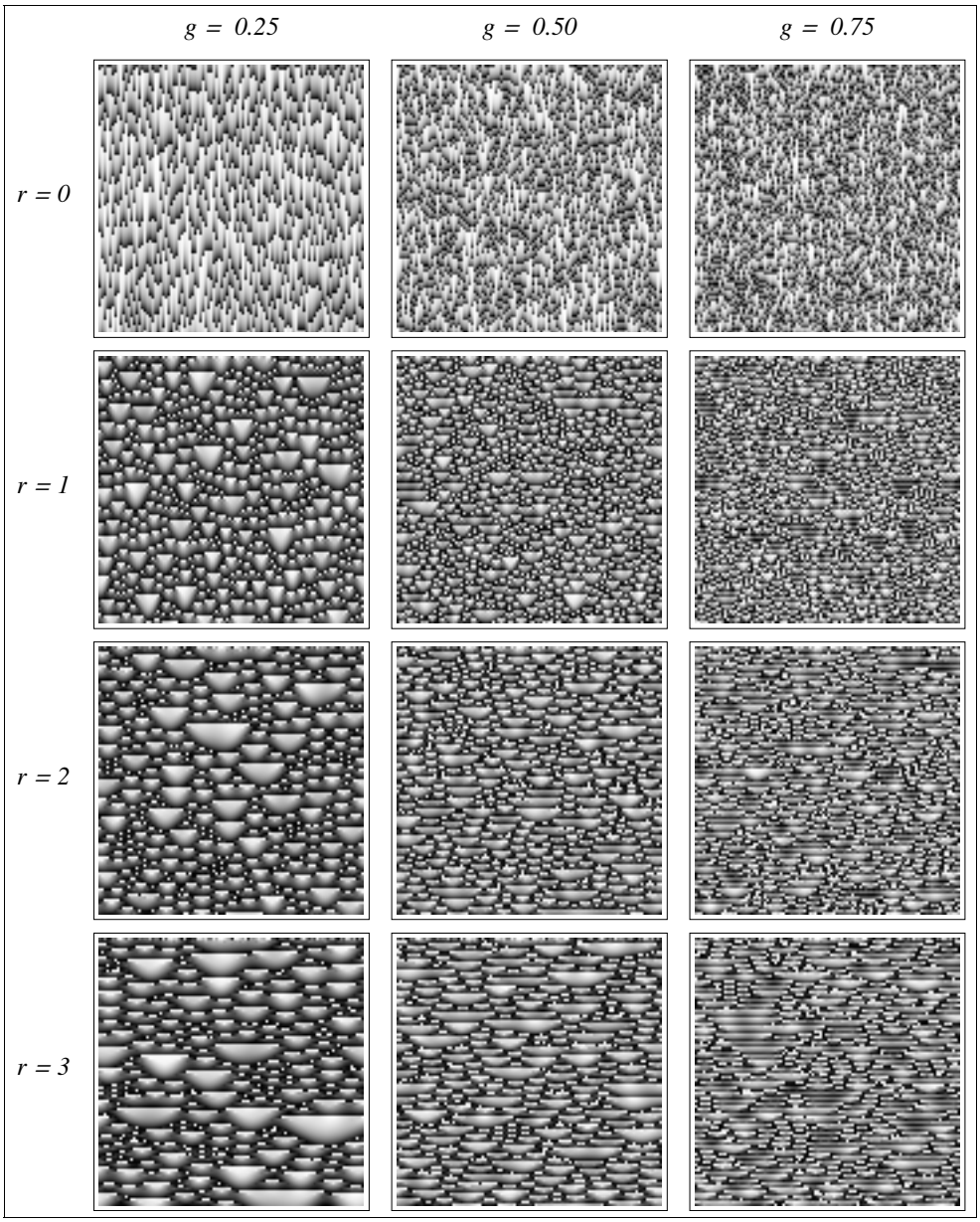

Figure 2. CCA model (4) of varying diffusion properties (r) at growth rates (g) as explained in Figure 1. Each panel has the same seed random initial cell biomasses distributed in 100 cells (n = 100). The vertical axes of each case represents computational steps (time), increasing downwards. The figure includes 100 computational steps (t=100).

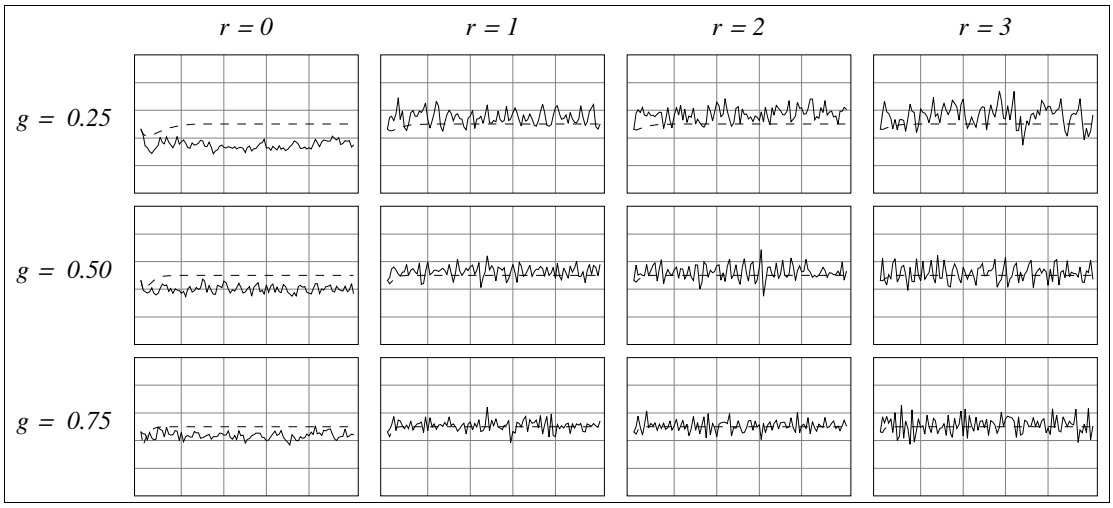

Figure 3. The solid curves represent biomasses over time derived by CCA model (4) of range parameter values (r) and growth rates (g) with the same seed random initial cell biomasses distributed in 100 cells (n = 100). The vertical axes of each case measures biomass and the horizontal axis time. The figure includes 100 computational steps (t=100). The dashed curves are biomasses derived by LCA model (7), the corresponding logistic growth functions.

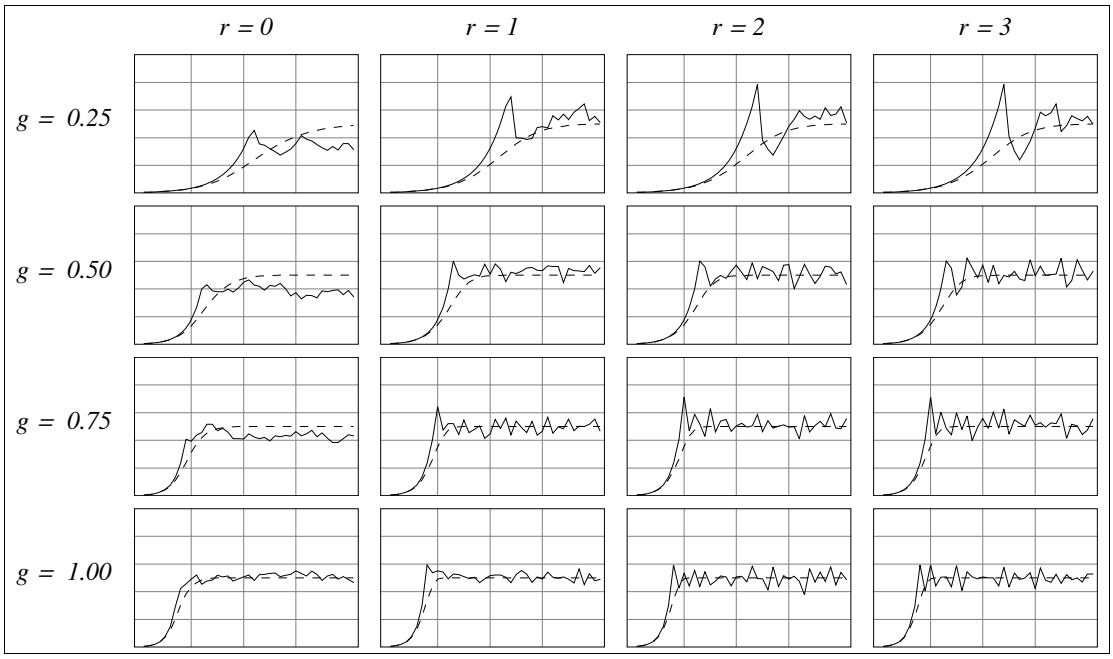

Figure 4. Biomasses over time in a CCA model (4) (solid curves) and LCA model (7) (dashed curves) of varying diffusion properties (r) at growth rates (g) with the same random initial cell biomasses and 100 cells (n = 100). The vertical axes of each case measures biomass and the horizontal axis time. The figure includes 100 time steps (t=100).

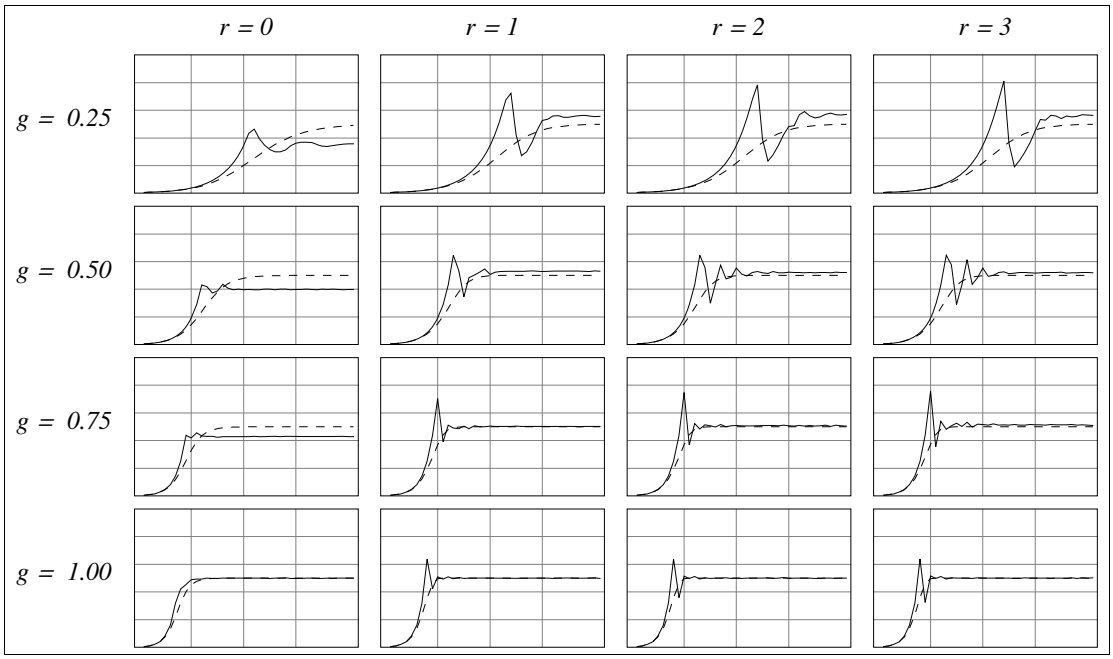

Figure 5. Biomasses over time in a CCA model (4) (solid curves) and LCA model (7) (dashed curves) of varying diffusion properties (r) at growth rates (g) with the same random initial cell biomasses and 100,000 cells (n = 100,000). The vertical axes of each case measures biomass and the horizontal axis time. The figure includes 100 time steps (t=100).

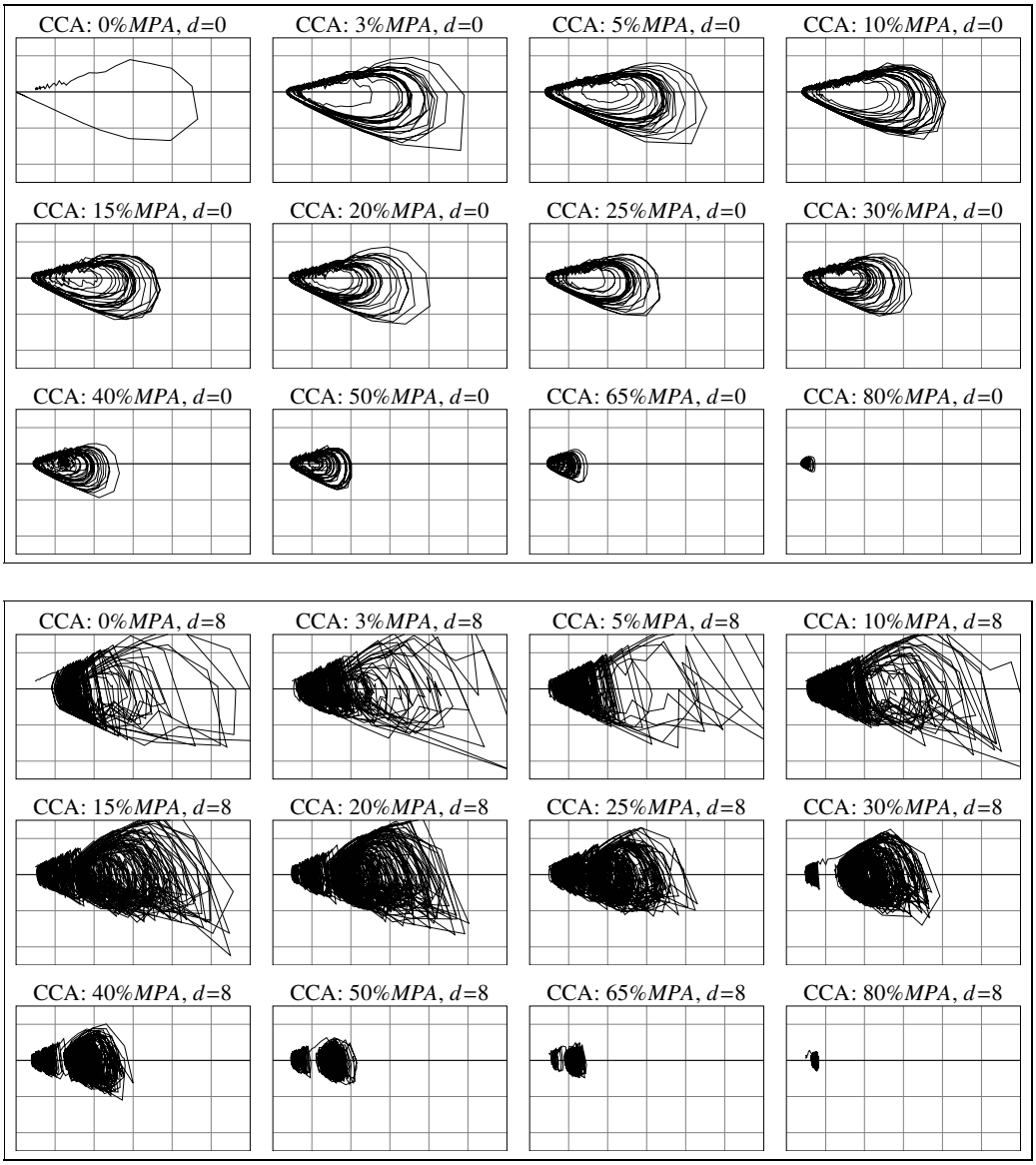

Figure 6. CCA model (17) on varying percentage of *MPA* cells and two fishing effort distribution, d=0 (upper panel) and d=8 (lower panel). Parameter values used are displayed in Table 3. In all graphs the horizontal axis measure total fishing effort (*E*), while net revenue (*NR*) is measured by the vertical axis. The period displayed in each graph counts 2000 time steps.

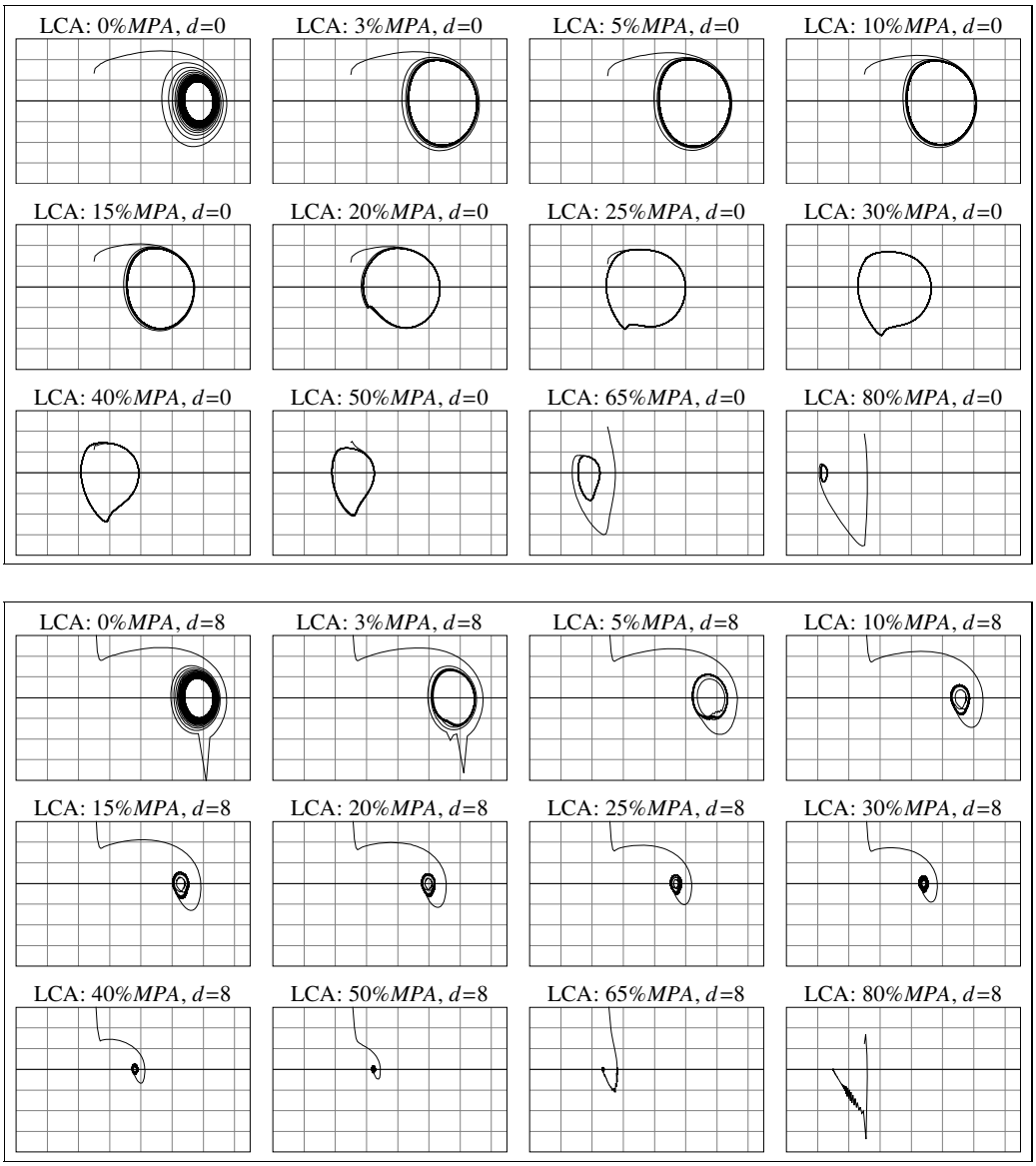

Figure 7. LCA model (19) on varying percentage of *MPA* cells and two fishing effort distribution, d=0 (upper panel) and d=8 (lower panel). Parameter values used are displayed in Table 3. In all graphs the horizontal axis measure total fishing effort (*E*), while net revenue (*NR*) is measured by the vertical axis. The period displayed in each graph counts 2000 time steps.

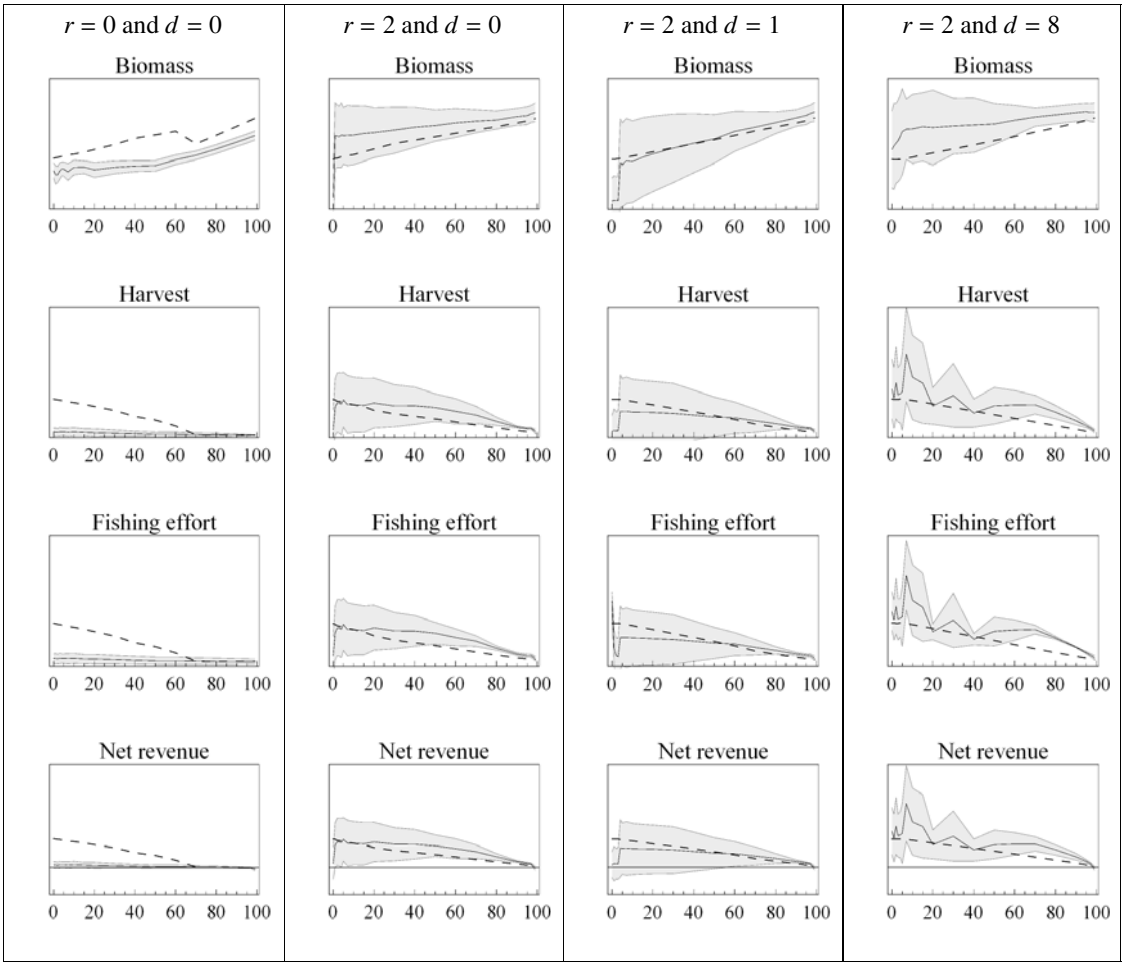

Figure 8. Average values of biomass, harvest, effort and rent obtained by *CCA* model (17) (solid curves) and *LCA* model (19) dashed curves for simulations over periods of 500 time steps. The shaded areas show the variances found in the *CCA* model (19). Parameter values are as dislayed in Table 3 unless other is indicated in plot labels where different r and d values are displayed.

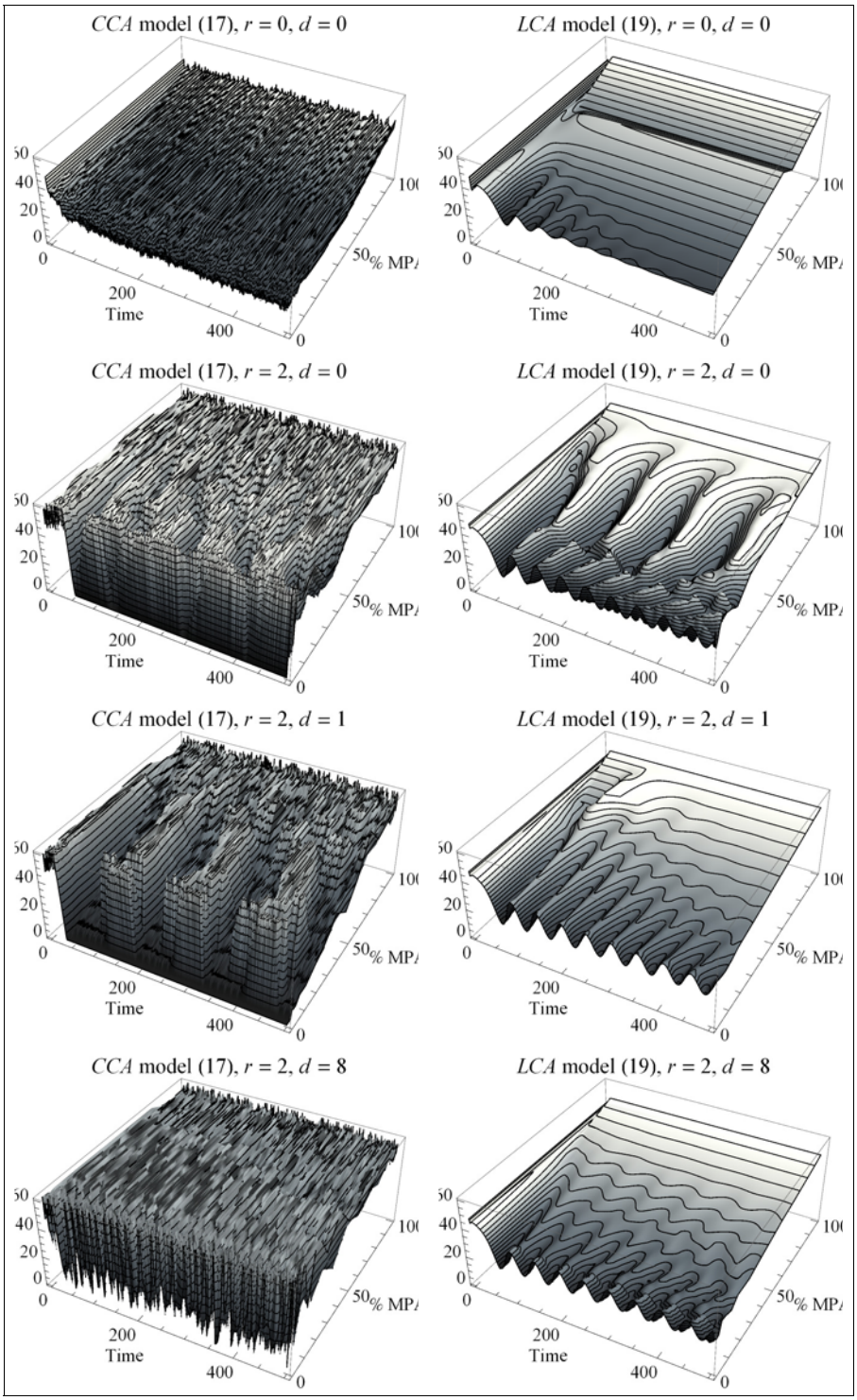

Figure 9. Surface plots of the biomasses calculated in Figure 8, as functions of *MPA* size and time. CCA model (17) is presented in the left column, while LCA model (19) is presented in the right column.

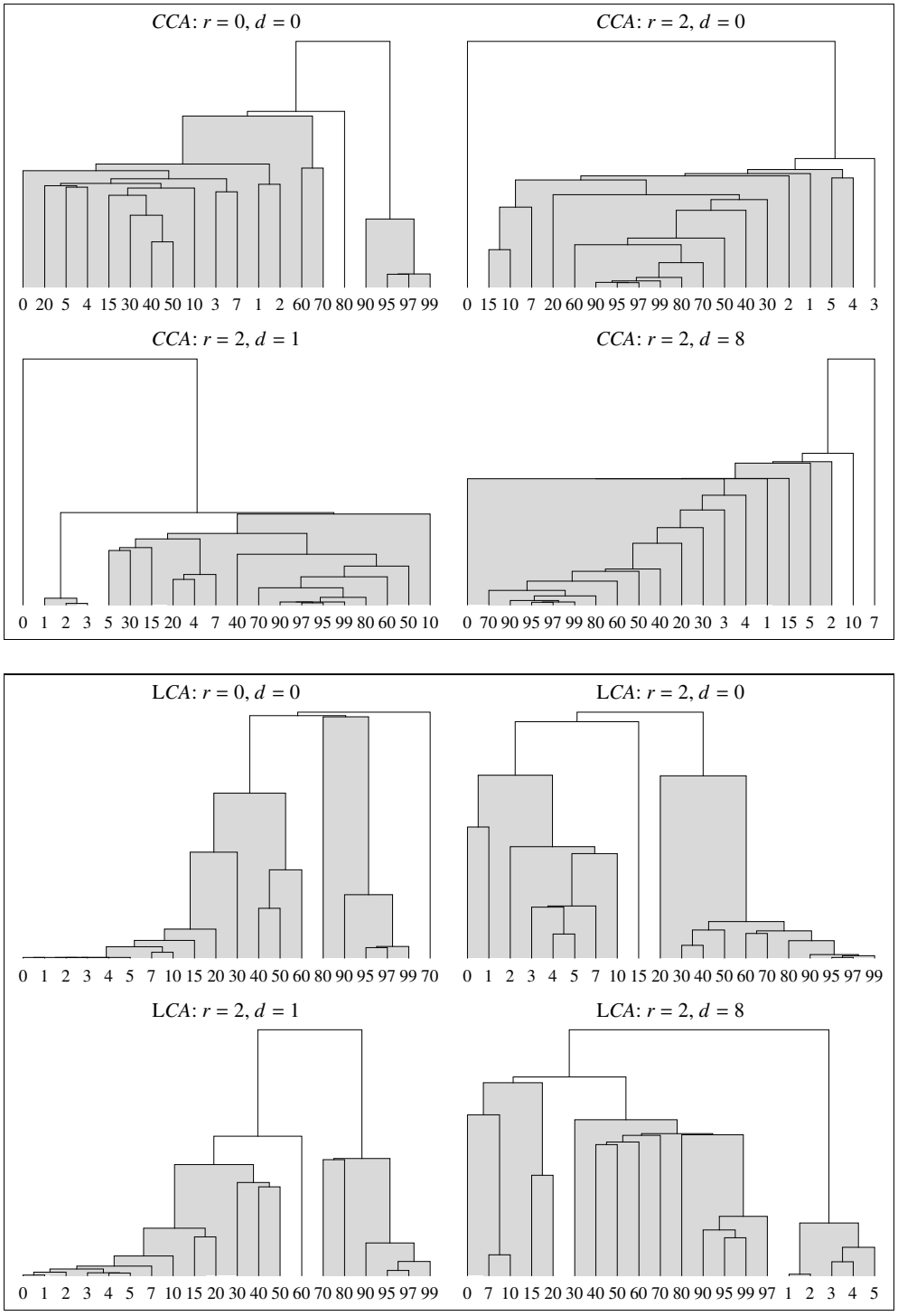

Figure 10. Dendrogram plots showing clustering on MPA size (horizontal axis) of the data sets presented in Figures 8 and 9. The upper panel shows clustering on MPA size in the CCA model (17), while the lower panel shows the corresponding clustering pattern in the LCA model (19). Data included in the cluster analyses are biomasses, fishing efforts and net revenues over the period of 500 time steps. The vertical axis indicates how close the sets of data belonging to each MPA size are, increasingly downwards.